A Time-and Temperature-Dependent Simulation of the GTO Turn-Off Process

Akio Nakagawa**
David H. Navon

**Toshiba Research & Development Center, 1 Komukai Toshibacho, Saiwai-ku, Kawasaki, 210, Japan
Department of Electrical & Computer Engineering, UMASS, Amherst, MA

Abstract

New insight into the GTO thyristor turn-off process has been obtained by performing an exact two-dimensional time- and temperature-dependent numerical simulation. Novel numerical solution techniques for faster convergence enable efficient modeling of high voltage operation as well as simultaneous electrical and thermal solutions. It was found that an additional current term relating to bandgap variation with temperature should be included.

The model was applied to a 200μmX5mm emitter GTO. A large current 34A(3,400A/cm^2) was turned-off by 6A of gate current. The peak current density, 17,000A/cm^2, was reached during the fall-time transient. The final on-region width (<50μm) was found to be a decreasing function of lateral gate current density. When the total anode current is high, an initial anode voltage increase is caused by the confinement of the on-region to a narrow area. The maximum applied voltage for the current crowded area was also found to be restricted by a mechanism similar to punch-through.

Introduction

Recent advances in the high power GTO thyristor development have enabled such devices to be operated at more than 1000A and 2500V [1]. However, only little efforts have been made for analyzing its SOA or failure mechanism [2,3]. The present paper tries to understand the plasma squeezing phenomena as well as failure mechanism, making use of numerical modeling.

Some current existing two-dimensional models are of a computer-time consuming nature, if four basic equations are solved simultaneously [4]. Coarse grid structure, inclusion of mobility derivatives associated with electrostatic potential, direct solution method, etc. enable efficient solution in practical computer-time.

Mathematical Model and Solution Method

Current equation A) thermal gradient

The current equation under nonisothermal conditions must include the current terms due to the thermal gradient. One of them is so called thermal diffusion and is expressed by [5].

$$qnD_T \frac{dT}{dX},\ D_T = \frac{k}{2q}\mu. \qquad \ldots(1)$$

The other current term is due to bandgap variation induced by the temperature gradient and is approximated by

$$-\frac{1}{2} q\mu_n n \frac{d\Delta Vg}{dX} = -q\mu_n ns\frac{dT}{dX}\ ;\ 2s = 2.82X10^{-4}\ [6] \qquad \ldots(2)$$

where it is assumed that both bandgap edges change by the same amount of sT. This term is opposite to the previous term and is larger.

B) Heavy-doping-effects and Fermi statistics

A characteristic parameter w_n is defined [7], using Fermi statistics for electrons:

$$n_0 \exp\left(\frac{1}{kT_0}(F_n + qw_n)\right) = \int_{-\infty}^{\infty} \frac{\rho dE}{1+\exp((E-F_n)/kT_0)};$$

$$n_0 = N_c \exp(-E_{c,0}/kT_0). \qquad \ldots(3)$$

Here, w_n expresses the effective bandgap change, taking into account the effect of Fermi statistics. The current equation is expressed in exactly the same form as the conventional one in spite of the degeneracy

$$J_n = \mu_n nkT_0 \frac{dn}{dX} - q\mu_n n \frac{d}{dX}(\psi_n + w_n). \qquad \ldots(4)$$

Further more merit will be given by the fact that the experimentally obtained bandgap change using the conventional equation is directly connected to the value w_n+w_p, where w_p is the corresponding parameter for holes.

The final electron current equation to be solved, thus, is given by

$$J_n = \mu_n kT\frac{dn}{dX} - q\mu_n n \frac{d}{dX}Veff, \qquad \ldots(5)$$

where $V_{eff} = \psi_n + (w_n + sT) - \frac{k}{2q}T$.

Solution method

If V_{eff} does not change rapidly, then dV_{eff}/dX can be regarded as constant between two grid points and the conventional discretization procedure can be used by replacing ψ by V_{eff}. An independent variable set (n,p,ψ,T) is used because of programing feasibility. There is almost no difference in the convergence rate even if another set is chosen.

In actual program, (n,p,ψ) are solved simultaneously by getting a triangular matrix using the Gaussian elimination (direct) method. The temperature equation is separately solved by Stone's

** He is currently staying at UMass/Amherst, MA as a Visiting Scholar.

CH1832-5/82/0000-0496 $00.75

method. Final simultaneous solutions are reached by iterating the above two solution procedures alternately at each time step. Mobility derivatives are incorporated using the adjacent seven grid points instead of five in order to improve the convergence rate for high voltage calculations. For example, the magnitude of the electric field at point n in Fig. 1 is calculated using the ψ's at B,E,F. The advantage of a direct solution method over SLOR is given by comparing the number of multiplications between the two programs:

$$N_X < \sqrt{1.4\ f}, \qquad \ldots(6)$$

where N_X and f stand for the grid number for one direction and the number of the required SLOR iterations, respectively. When a 7X55 grid structure is chosen, the direct method is faster than SLOR if f > 35.

Results from the 2-Dimensional Model

In Fig. 1, the circuit condition and the device doping profile are given. The boundary surfaces for the temperature equation are also given by the dotted lines in the figure, where ideal heat-sinks (300K) are assumed.

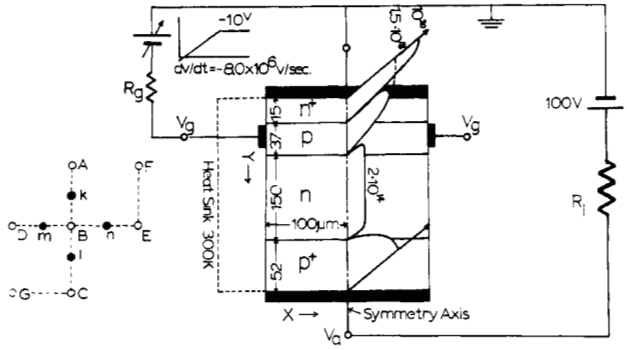

Fig. 1 Schematic diagram for the analyzed system

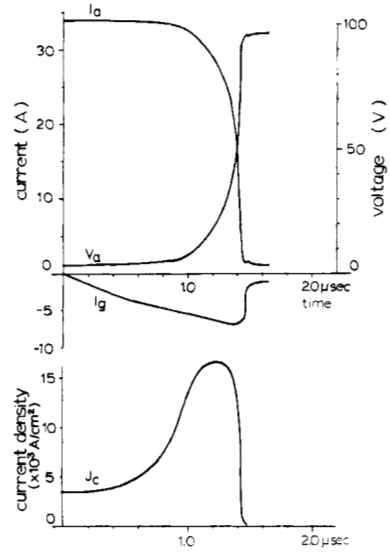

Fig. 2 Calculated current-voltage waveforms and current density change at device center

The model was applied to a GTO having a 200μm x5mm N^+ -emitter which conducts 34A at the voltage drop of 3.3V. The modeled GTO is one of the emitter island of a 600V, 600A Toshiba GTO. The initial current density can be as high as 3,400A/cm^2 since it was found [8] that the current usually concentrates into a small number of GTO elements during the turn-off process.

Fig. 2 shows the calculated waveforms of anode voltage, anode current and gate current. A storage-time of 1.1μsec and a fall-time of 0.3μsec are observed. Fig. 2 also shows the current density change for the middle junction at the device center. The highest current density (17,000A/cm^2) is achieved at the early fall-time period of t=1.26μsec and V_a=23.5V. It is true [2] that the highest current density appears at the end of fall-time for a low current case. However, in the case that high current is turned-off, reduction of the size of conduction area itself, causes a significant increase in the device voltage because a high anode voltage is necessary to conduct an extremely high current density. This fact leads to a substantial anode current decrease for a purely resistive load case, and will be confirmed later.

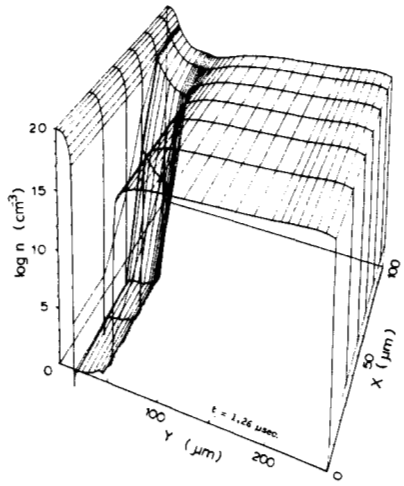

Fig. 3 Electron density distribution(t=1.26μsec.)

Fig. 3 shows the electron density distribution at t=1.26μsec. Most of the excess carriers in the p-base have been extracted already and only the narrow central portion (50μm) conducts all of the current. A tiny carrier hill is seen in the device center in Fig. 3, corresponding to the temperature increase there. It is a surprising fact that the quantity of the carriers in the n-base remains almost unchanged even for the turned-off portion so that the current in the n-base flows still uniformly as shown in Fig. 4, minimizing local heating. It should also be noted that in the n-base, a part of the current becomes lateral gate current so that the highest current density appears at the center of the middle junction.

Fig. 5 shows the ψ distribution for t=1.26μsec. It is seen that a channel for current flow is formed only at the device center, where the gate-cathode junction is forward biased.

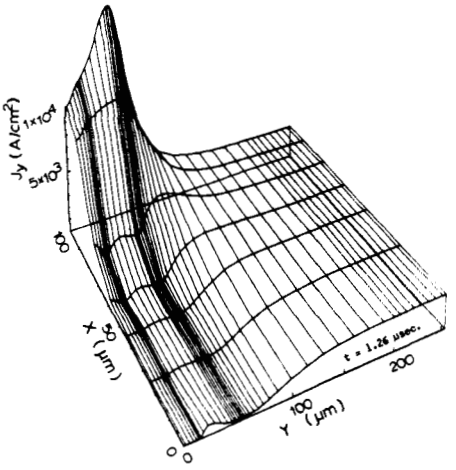

Fig. 4 Y-component of the current density distribution (t=1.26μsec.)

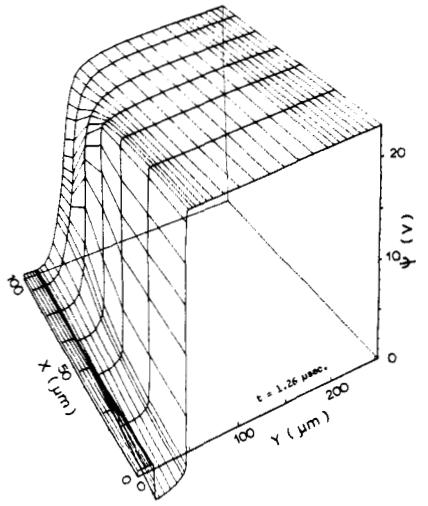

Fig. 5 Electrostatic potential (t=1.26μsec.)

Fig. 6 shows the temperature distribution at t=1.47μsec. A 20 degree temperature increase is seen in the highest current density area. The system behaves almost adiabatically because almost all of the heating occurs within 1μsec. Fig. 7 shows the electron density distribution at t=1.43μ sec. It is seen that the lateral carrier density gradient in the p-base has become less steep than in Fig. 3, corresponding to a derease in gate current density.

Fig. 8 shows the lateral carrier density distributions along X=19μm in the p-base. The carrier density gradient is very steep because of the high lateral gate current density (3,000A/cm^2 at t=1.26μsec.) and because of the reduced carrier diffusion length due to carrier-carrier scattering and a temperature increase. As the lateral

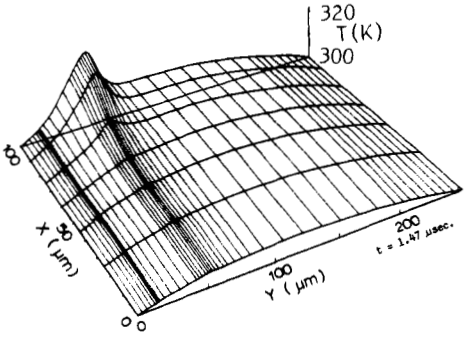

Fig. 6 Temperature distribution(t=1.47μsec.)

electron current at the edge of the conduction area is almost negligible, a high carrier gradient must exist to afford a lateral hole current. The transition region is as narrow as 10μm.

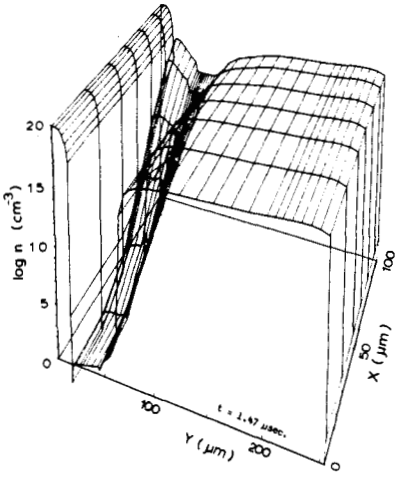

Fig. 7 Electron density distribution(t=1.47μsec.)

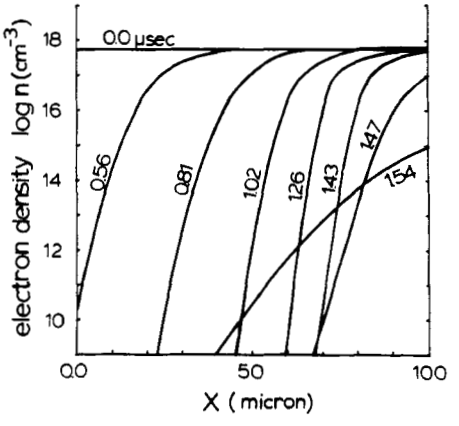

Fig. 8 Electron density distribution for X=19μm along X-axis for various time steps.

From t=1.02μsec., the conduction area continues to reduce while the anode voltage begins to increase rapidly and peak current density still increases. This represents a remarkable difference from the low current case [2], leading to the previously stated concept, and also verifying the assumption which was used in [3] for a 1-dimensional gate turn-off model.

Analysis from 1-Dimensional Model

This section is an extension of the work of paper [3], and attempts to understand the cause for the current concentration into a small portion of GTO in the turn-off process. This phenomena is basically 3-dimensional and even a 2-dimensional model is not fully applicable. A 1-dimensional model will be used with the same assumption as [3]. The results obtained can be regarded as characteristic of the current crowded region.

Fig. 9 shows steady-state I-V characteristics of several GTO's. A comparison between A and D gives a large current density difference which is caused merely by the added 2μm emitter depth.

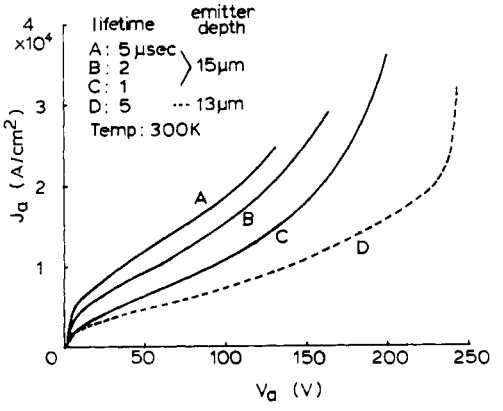

Fig. 9 1-dimensional simulation of the large current I-V characteristics (steady-state, I_g=0.0)

Fig. 10 shows the current density changes with time when various gate current densities are assumed. The current density is actually plotted against anode voltage, which is raised at the rate of 200V/μsec. A significant current density difference is also caused by a little difference in the gate current. It is expected that p-base sheetresistance difference can be a significant cause for the current concentrating into a small region. For example, a 20% difference in sheet-resistance (which is very likely) may cause almost the same amount of current density difference as that between A and D in Fig. 9, in the early stage of the anode voltage increase period during the turn-off process. In addition, 20% less gate current may be supplied to the higher current conducting area where the p-base sheetresistance is 20% higher than the other part of the emitter, resulting in the larger current concentration in this area.

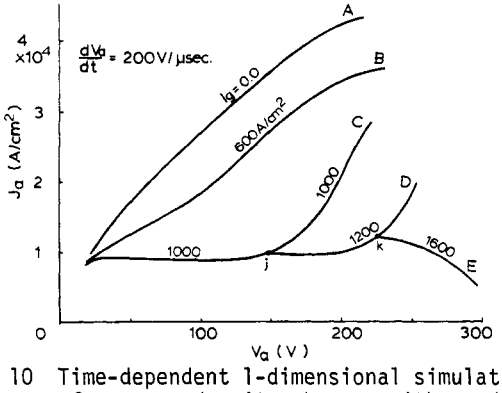

Fig. 10 Time-dependent 1-dimensional simulation of current density changes with anode voltage for various gate current densities

Other interesting phenomena are seen also in Figs. 9,10. For above 200V, the anode current density begins to increase rapidly. As the anode voltage increases, a high electric field region develops around the center junction. In the high electric field region, current flows mainly by drift so that the current ratio J_n/J_p is almost the same as that of μ_n/μ_p (assuming high injection condition n ≃ p). This ratio gradually decreases with electric field magnitude above $1X10^4$V/cm. Therefore, the electric field magnitude is determined by the ratio of J_n/J_p and does not change significantly. But the width of the high electric field region expands toward the p-emitter as the applied voltage increases (refer to Figs. 7,8 in [3]). If the supplied gate current is insufficient then the high electric field region approaches the p-emitter and causes a high hole diffusion current, resulting in the current density increase in this area. The recent experiment by T. Nagano et al. [2] showed that the maximum interruptable current significantly decreases with the increase in applied voltage over 400V for a 700V device. This voltage is very close to the voltage where the above stated phenomena occurs and which is roughly predicted to be around $2X10^4W_{NB}$(V) where W_{NB} is the n-base width (cm).

Acknowledgment

The authors wish to thank Dr. T. W. Tang for useful discussions. One of the authors thanks Toshiba Corporation for providing the opportunity for this work and his stay in the U.S.A. A part of this work is from the joint-research of H. Ohashi and one of the authors.

References

[1] M. Azuma et al, IEEE Trans. ED-28, 270 (1981)
[2] T. Nagano et al, 1982 PESC, pp 383.
[3] H. Ohashi et al, 1981 IEDM Tech. Digest,pp414.
[4] V.C. Alwin et al, IEEE Trans. ED-24,1297(1977)
[5] R. Stratton, IEEE Trans. ED-19,1288(1972)
[6] G.G. MacFarlane et al, Phys. Rev. 111,1245 (1958)
[7] A. Nakagawa, Solid-St. Electron, 22,943(1979)
[8] T.C. New et al, IEEE Trans. ED-17,706(1970)